Nuclear Instruments and Methods in Physics Research B 269 (2011) 1572–1577

Contents lists available at ScienceDirect

Nuclear Instruments and Methods in Physics Research B

journal homepage: www.elsevier.com/locate/nimb

Desorption of large molecules with light-element clusters: Effects of cluster size and substrate nature

Arnaud Delcorte [a,*], Barbara J. Garrison [b]

[a] Institute of Condensed Matter and Nanosciences – Bio & Soft Matter, Université catholique de Louvain, Croix du Sud, 1 bte 3;B-1348 Louvain-la-Neuve, Belgium
[b] Department of Chemistry, Penn State University, University Park, PA 16802, USA

ARTICLE INFO

Article history:
Received 27 July 2010
Received in revised form 4 November 2010
Available online 13 December 2010

Keywords:
SIMS
Massive cluster impact
Desorption
Sputtering
Molecular ion
Polymers
Molecular dynamics
MD
Computer simulations
Kiloelectronvolt

ABSTRACT

This contribution focuses on the conditions required to desorb a large hydrocarbon molecule using light-element clusters. The test molecule is a 7.5 kDa coil of polystyrene (PS61). Several projectiles are compared, from C_{60} to 110 kDa organic droplets and two substrates are used, amorphous polyethylene and mono-crystalline gold. Different aiming points and incidence angles are examined. Under specific conditions, 10 keV nanodrops can desorb PS61 intact from a gold substrate and from a soft polyethylene substrate. The prevalent mechanism for the desorption of intact and 'cold' molecules is one in which the molecules are washed away by the projectile constituents and entrained in their flux, with an emission angle close to ~70°. The effects of the different parameters on the dynamics and the underlying physics are discussed in detail and the predictions of the model are compared with other published studies.

1. Introduction

In secondary ion mass spectrometry (SIMS), relatively small polyatomic ions such as SF_5^+ and C_{60}^+ were among the first cluster projectiles to be used successfully for 3D molecular characterization of solid organic samples [1,2]. At the other end of the spectrum, massive clusters and nanoparticles are also apt to produce high mass molecular information (Au_{400} [3], Ar_n [4,5], nano- and microdroplets used in desorption electrospray ionization – DESI [6,7] and related techniques [8–10]). Recently, it was even shown that large noble gas clusters [11,12] and, to a certain extent, charged water droplets [13,14], could also be successfully used for molecular depth-profiling.

For mass spectrometric analysis and imaging of organic samples, suppression or tunable reduction of sample fragmentation is desirable. In the case of Ar_n cluster bombardment of arginine, leucine and triglycine films, reduced fragmentation could be attained by increasing cluster size for a given acceleration energy (from Ar_{300} to $Ar_{1500-2000}$) [4,5]. Theoretically, a transition between soft desorption and fragmentation was also predicted for large Ar_n cluster bombardment of monolayers of benzene and polystyrene on silver [15]. However, experimental results obtained with 40 keV Ar_n clusters (between Ar_{200} and Ar_{10000}) show that the sputtering yields decrease with increasing cluster size [16,17]. A similar effect was observed with organic samples, namely, arginine crystals [4]. For van der Waals solids bombarded by the same Ar_n clusters with ~15 and ~40 keV of kinetic energy, molecular dynamics (MD) simulations by Anders et al. predict a similar decrease of the sputtering yield beyond $n = 10$ [18]. The bombardment of organic samples by a series of carbon (from 0.1 to 2.2 kDa [19]) and hydrocarbon projectiles (from 0.3 to 110 kDa [20]) was also studied theoretically. Simulations of benzene crystals bombarded by fullerenes (up to C_{180}) indicated a trend of decreasing yield with nuclearity at low energy (5–10 keV) [19]. A yield decrease was even more clearly demonstrated for projectiles larger than 2 kDa bombarding polymeric materials with similar energies [20]. In the case of 1.4 kDa polyethylene (PE) oligomer molecular samples, 10 keV bombardment with the largest organic projectiles (110 kDa, still much smaller than DESI droplets) did not lead to any desorption at all, despite the formation of a wide crater in the surface [20].

In summary, if large cluster projectiles have the advantage to reduce fragmentation and, therefore, have a certain potential for soft molecular desorption, the range of initial conditions (projectile size, energy, angle, substrate nature, etc.) in which such desorption is possible and the relevant physical parameters are not well

* Corresponding author.
E-mail address: arnaud.delcorte@uclouvain.be (A. Delcorte).

0168-583X/$ - see front matter © 2010 Elsevier B.V. All rights reserved.
doi:10.1016/j.nimb.2010.11.023

identified yet. Hereafter, we explore the conditions required to desorb a large hydrocarbon molecule from hard (Au) and soft (PE) substrates using massive light-element clusters. The influence of different parameters is tested (cluster size, impact point, incidence angle). In the case of molecular emission, our predictions provide quantities (sputtered molecule energy and angle) that could be tested in future experiments.

2. Computational method

The molecular dynamics (MD) simulation program used in this study is the SPUT code developed at Penn State University for sputtering applications [21,22]. In the classical MD method, Hamilton's equations of motion are numerically integrated over some time interval, providing us with the position and velocity of each particle at each timestep. Forces among the atoms or particles in the system are derived from empirical interaction potentials.

The molecular projectiles used in this study are coronene, C_{60}, polystyrene oligomers (PSX with $X = 4,16,61$ repeat units) and a series of $(PS4)_y$ oligomer molecular clusters ($y = 4$, 16, 34, 66, 197) [23]. All the projectiles were modeled at the atomistic level, with hydrogen ^1H replaced by tritium ^3H for computational efficiency.

The first sample is a crystal of gold containing 4.8×10^5 atoms, with a polystyrene molecule (PS61, 990 atoms; ~7.5 kDa) adsorbed in the center of the Au(1 1 1) surface. The second sample is an amorphous polyethylene substrate with five PS61 molecules adsorbed on its surface (four molecules placed at the corners of a square and at ~5 nm from the central molecule). In order to reduce computational expense, the atoms of the PE molecules were grouped to form united atoms or particles (coarse-graining, CG). Each PE oligomer is a string of 97 CH_2 particles of 14 Da capped with two CH_3 particles of 15 Da. The PE substrate, made of $\sim 4.1 \times 10^5$ united atoms, is fully described in Ref. [24]. The binding energy of a PS61 molecule to the Au substrate is 1.8 eV and to the PE substrate, 8.2 eV.

The forces between the atoms are derived from empirical potentials. Those are the MD/MC-CEM potential for Au–Au interactions [25], the AIREBO potential for the C–C and C–H interactions within the hydrocarbon projectiles and the PS61 molecule [26,27], the Lennard–Jones potential for the intermolecular interactions and the Morse potential for the intramolecular interactions in PE (see Ref. [24] for the parameters). The Lennard–Jones potential were also used to describe the Au–C and Au–H interactions, with ε and σ parameters respectively equal to 0.00277 eV and 3.172 Å for Au–C interactions and 0.00179 eV and 2.746 Å for the Au–H interactions [28,29]. These values of binding energy, used to describe nonbonding (van der Waals) interactions between the Au surface and the C, H atoms of the PS molecule, are probably not adequate to account for the binding of single Au atoms and small Au clusters with carbon and hydrocarbon species. A weak Lennard–Jones potential was used between the atomistic C,H atoms and the CG CH_x particles of the molecular sample [20].

In all the simulations, the total kinetic energy of the projectiles was 10 keV. The incidence angles and the aiming points were variable (See Table 1). One realistic molecular conformation was tested and one single trajectory was computed for each set of energy, angle and target region. Indeed, in contrast with the stochastic nature of the collision cascade processes [30], bombardment with large polyatomic projectiles is a mesoscopic event and little fluctuations in sputtering are expected, depending on the exact impact point and molecular conformation [21]. The simulations were run for up to 30 ps total time. A friction region at 0 K and a rigid layer were defined at the bottom and sides of the sample in order to absorb the pressure waves induced by the projectiles [31].

Table 1
Summary of the effects of the different impact conditions on the target molecules.

Angle (°), [distance (nm)]	Desorption	Mechanism	Angle	C-o-M KE (eV)	Internal KE (eV)
Au substrate 0°	YES	Spring	12°	5.4	184
15°	YES	Spring	24°	7.6	185
30°	YES	Spring	56°	13	202
45°	NO	Spring/Washing	>85°	–	–
60°	NO	Washing	>85°	–	–
0°, 5.8 nm	YES	Washing	67°	48	41
0°, 8.7 nm	YES	Washing	70°	15	26
0°, 11.6 nm	NO	Washing	>85°	–	–
PE substrate 0°	NO	Pushing down	–	–	–
0°, 5.0 nm	NO	Lifting	–	–	–
[a]60°,**1**, 9.9 nm	YES	Washing	81°	171	219
[a]60°,**2**, 5.0 nm	YES	Washing	66°	49	143
[a]60°,**3**, 3.5 nm	YES	Washing	67°	35	71
[a]60°,**4**, 0.0 nm	NO	Pushing down	–	–	–

[a] The second number refers to the molecule labels in Fig. 3.

3. Results and discussion

3.1. Bulk polymer substrate

Before looking in detail into desorption of PS61 oligomers adsorbed on gold and polyethylene, Fig. 1 summarizes the sputtering results obtained for bare polyethylene substrates bombarded by 10 keV hydrocarbon projectiles. The mass sputtered as intact molecules and as fragments is presented as a function of energy/nucleon, and velocity, which were found to be the relevant parameters influencing the sputtering yields. The results obtained with all the clusters fit on one line that tends to zero around 0.1 eV and exhibits a plateau between 2 and 40 eV. The plateau at high energy/nucleon (i.e. small cluster size) means that the sputtering yield becomes independent of nuclearity, while the other side of the curve indicates a pronounced influence of nuclearity for a given total energy. These results support the experimentally observed yield decrease with projectile size for a given acceleration energy.

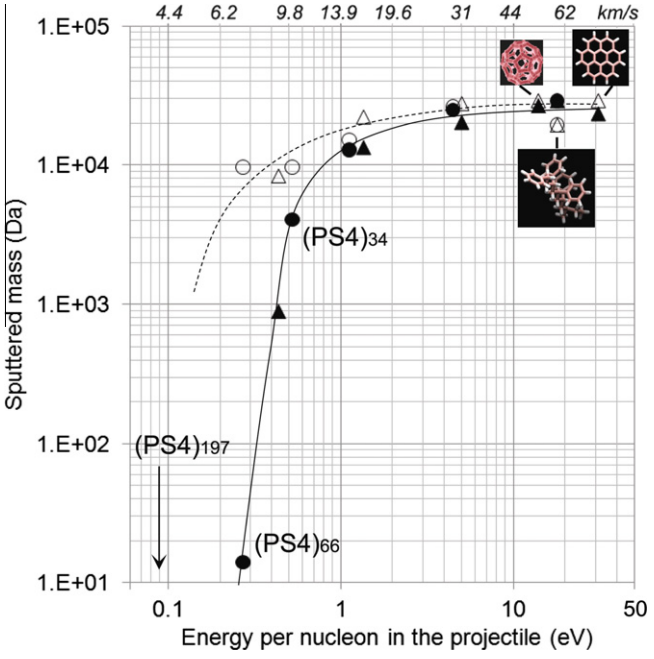

Fig. 1. Mass sputtered as intact molecules (open symbols and dashed line) and as fragments (full symbols and full line) for amorphous PE samples under 10 keV cluster bombardment (0° incidence). *Circles:* $(PS4)_n$ clusters. *Triangles:* other light-element clusters.

With 10 keV of kinetic energy, the most massive cluster used in these simulations, $(PS4)_{197}$, is unable to sputter polyethylene.

A reduction of fragmentation with decreasing energy per nucleon is also predicted for hydrocarbon molecular clusters. Below ~1 eV/nucleon, fragmentation of the sample is minimal with yet significant molecular emission yields. Because large intact molecule detection is desirable for certain applications of organic mass spectrometry, the rest of this study focuses on the conditions that must be met for such massive clusters with energies below 1 eV/nucleon to desorb a 7.5 kDa polystyrene molecule.

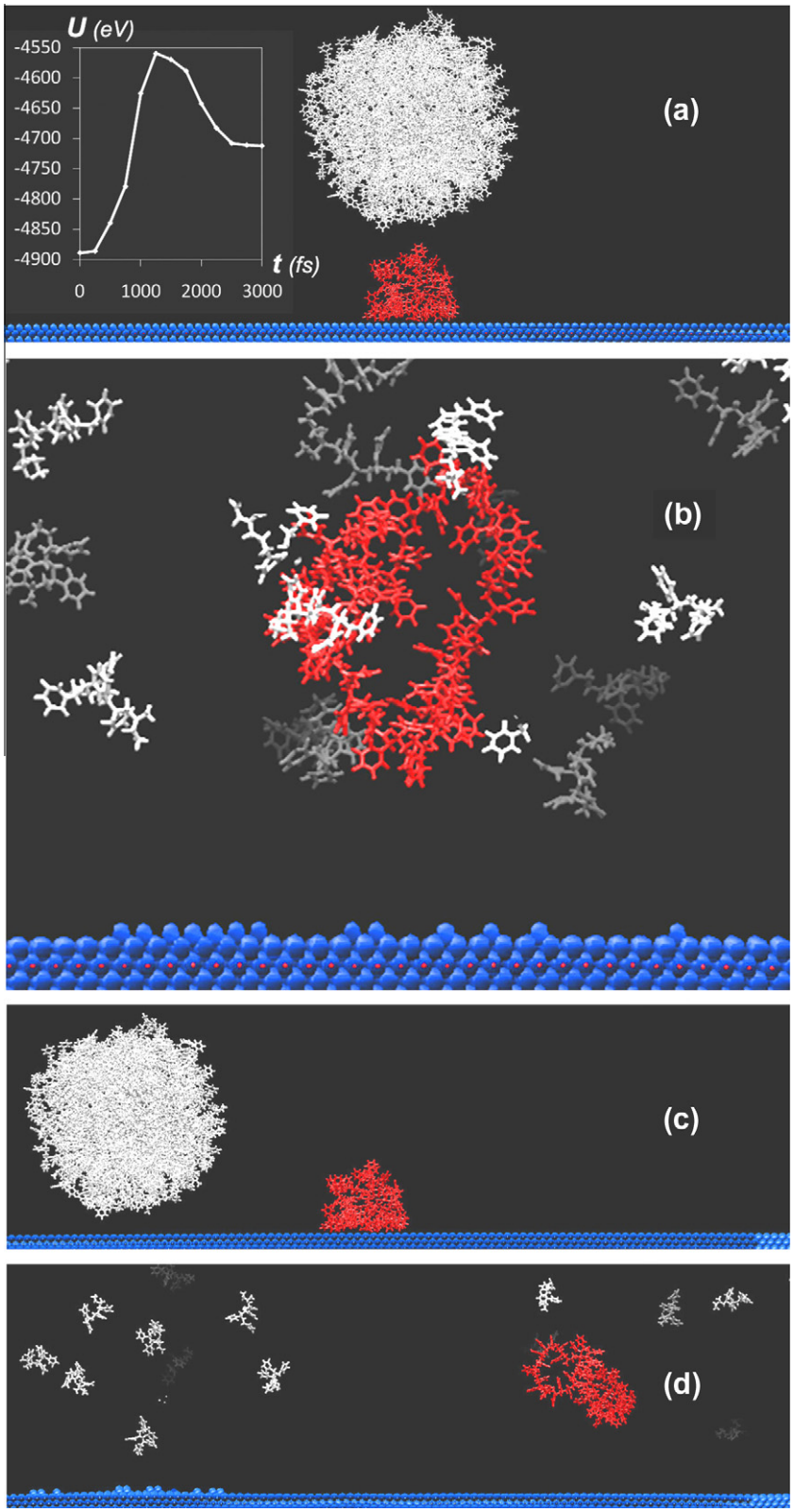

Fig. 2. Desorption of a PS61 molecule (red) from a Au(1 1 1) substrate. *Projectile:* 10 keV $(PS4)_{197}$ organic nanodrop (white); (a–b) direct hit, 0° incidence, 0 and 12 ps; (c–d) side hit, 0° incidence, 0 and 17 ps. *Inset of (a):* Potential energy (U) of PS61 as a function of time (t). (For interpretation of the references to colour in this figure legend, the reader is referred to the web version of this article.)

3.2. PS molecule adsorbed on heavy metal

In order to explore the conditions of intact molecule desorption under massive cluster bombardment, 7.5 kDa polystyrene oligomers, PS61, were placed first on a Au(1 1 1) substrates and different sets of bombardment parameters were tested. The main observations are summarized in the first part of Table 1 and Fig. 2.

For 10 keV $(PS4)_{197}$ bombardment (0.09 eV/nucleon), we distinguish two major interaction mechanisms, depending on whether the velocity vectors of the molecules of the projectile have a normal or a markedly off-normal (>45°) orientation when they reach the PS61 molecule. In the first case, i.e. when the projectile hits PS61 directly with an incidence of 0–30°, the molecule is compressed (up to 330 eV potential energy increase, see inset of Fig. 2a) on the rigid substrate and then reacts like a spring, gaining enough translational energy to desorb ('spring' mechanism, Fig. 2a–b). The limiting case is at 45°, when the momentum gained by the molecule is oriented very close to the surface plane and the translational energy is insufficient to overcome the surface binding and lift it up. Then the molecule appears to unfold and creep on the Au substrate. An increase of the total projectile kinetic energy should lead to an increase of the molecule compression in the vertical direction for a given angle and, therefore, to a larger limit angle for desorption. However, by increasing the energy per atom in the projectile, it should also increase the fragmentation probability. In this respect, our calculations show that bombardment with 10 keV $(PS4)_{66}$ at normal incidence (0.27 eV/nucleon) induces the fragmentation of the molecule and the ejection of its fragments via the same 'spring' mechanism (not shown).

The second mechanism dominates when the projectile hits the molecule directly with a velocity vector angle >45° or if it hits with normal incidence at some distance of the molecule ('washing' mechanism, Fig. 2c–d). In the latter case, the PS4 molecules splash on the Au substrate and their velocity vectors are redirected almost parallel to the surface before they impact PS61. For the normal bombardment, three impact points, located at 6, 9 and 12 nm of the PS61 molecule center of mass (C-o-M), were tested in order to verify the effect of the distance between the impact and the molecule on the molecular emission. The results show that the momentum transferred to PS61 is sufficient to desorb it if the impact point is at 6 and 9 nm of the molecule C-o-M but not if it is at 12 nm. Note that, in these simulations, the binding energy between the metal surface and the molecule, only accounting for nonbonding interactions, is relatively low (~2 eV). A larger binding energy should lead to a reduced emission probability.

The 'spring' mechanism produces angles of emission that are closer to normal than the 'washing' mechanism (strongly off normal, ~70°). The kinetic energies (KE) of the departing molecules were calculated in each case (Table 1). The 'spring' mechanism generates molecules with a low translational KE (~10 eV) and a high internal KE (~200 eV), i.e. 'hot' molecules that will be prone to unimolecular dissociation reactions. In the case of the 'washing' mechanism, the translational KE is larger (15–50 eV) and the internal KE is much lower (<50 eV). Therefore, molecules desorbed by the 'washing' mechanism will have much greater chances to remain intact until they reach the detector in a real experiment.

The desorption mechanisms of PS61 described in Fig. 2 can be compared with the case of much smaller PS4 molecules (0.6 kDa), adsorbed on Ag (1 1 1) and bombarded by 15 keV Ar_{2953} (118 kDa, close to the mass of $(PS4)_{197}$) [15]. First, the 'trampoline' mechanism described by Rzeznik et al. leads to almost normal emission from under the projectile, like our 'spring' mechanism. However, in our case, the deformation of the heavy Au substrate is very limited and the energy that is transferred into C-o-M translation of the molecule mostly comes from the potential energy stored *in the molecule* (not in the substrate), leading to very large internal energies. The second process identified under Ar_{2953} impact is very close to our 'washing' mechanism. One difference is that PS61, much larger than PS4, does not need a neighbor molecule that could play the role of a 'takeoff board' such as was described in [15]. PS61 is quasi-spherical and much larger than PS4. Therefore, when the projectile hits the substrate near the molecule, portions of the projectile reflected from the substrate can directly transfer momentum with a significant vertical component ('pure' washing, Fig. 2c–d). On the other hand, when the projectile hits the molecule directly with an off-normal incidence, the horizontal component of the momentum induces the washing effect while the downward component transfers energy in the internal modes (mixed mechanism, not shown). The washing effect was also observed upon bombardment of irregular Si surfaces by 20 keV Ar_{2000} clusters [32,33]. Despite the differences in the projectile and substrate properties, two remarkable similarities can be noticed: (i) for a strongly off-normal incidence (80°), most of the irregular structure adsorbed on the surface is entrained as a single piece; (ii) the angle of ejection increases with the distance between the impact point and the structure position, up to a point where no ejection occurs (redeposition when the distance is larger than 10 nm, analogous to our results) [32]. These studies also show that structures larger than the projectile and bonded to the surface cannot be desorbed, only deformed.

3.3. PS molecule adsorbed on polyethylene

For the study of molecular emission from a soft material, the same amorphous PE sample used to gather the results of Fig. 1 was chosen as a substrate for PS61. The main results, obtained upon various bombardment conditions, are summarized in the second part of Table 1 and Fig. 3.

With this projectile size and total energy (10 keV), it seems impossible to desorb PS61 from the soft PE substrate under normal incidence (Fig. 3a–b). This result is consistent with the observations made for the pure PE sample (Fig. 1). Complementary simulations show that 10 keV $(PS4)_{66}$ projectiles are also unable to desorb PS61 molecules in this configuration. In contrast, 10 keV C_{60} impacts induce their complete unfolding and, eventually, their emission (not shown). Nevertheless, with massive $(PS4)_{197}$ clusters, changing the incidence angle from 0° to 60° allows us to recover some emission, with a desorption process that is quite similar to the aforementioned 'washing' mechanism (Fig. 3c–e). Here again the lateral momentum is transferred by the projectile, but the way the vertical momentum is obtained is more complex than for the rigid surface. It is actually due to a combination of energy storage in the molecule and deformation of the substrate. In Fig. 3d–e, it is the slope of the forming crater that acts as the 'takeoff board' for molecules 1 and 2. The motion is further complicated by the interaction with the substrate molecules that remain linked to the PS molecule for a long time. Note that the molecule that was at the impact point (number 4) is simply crushed and pushed down in the forming crater.

In this case again the 'washing' mechanism desorbs molecules with an angle of ~70°, much like what was observed with the gold substrate. The internal KE of the departing molecules, however, tends to be larger, but it is also very dependent on the distance between the impact point and the considered molecule. Quite surprisingly, both the translational and the internal KE increase with increasing distance from the impact up to 10 nm. The detailed analysis of the trajectory provides two indications to explain this effect: (i) because molecules 4, 2 and 1 are on a straight line and aligned with the projectile trajectory, they are entrained with the projectile and, in addition, energy is transferred from one molecule

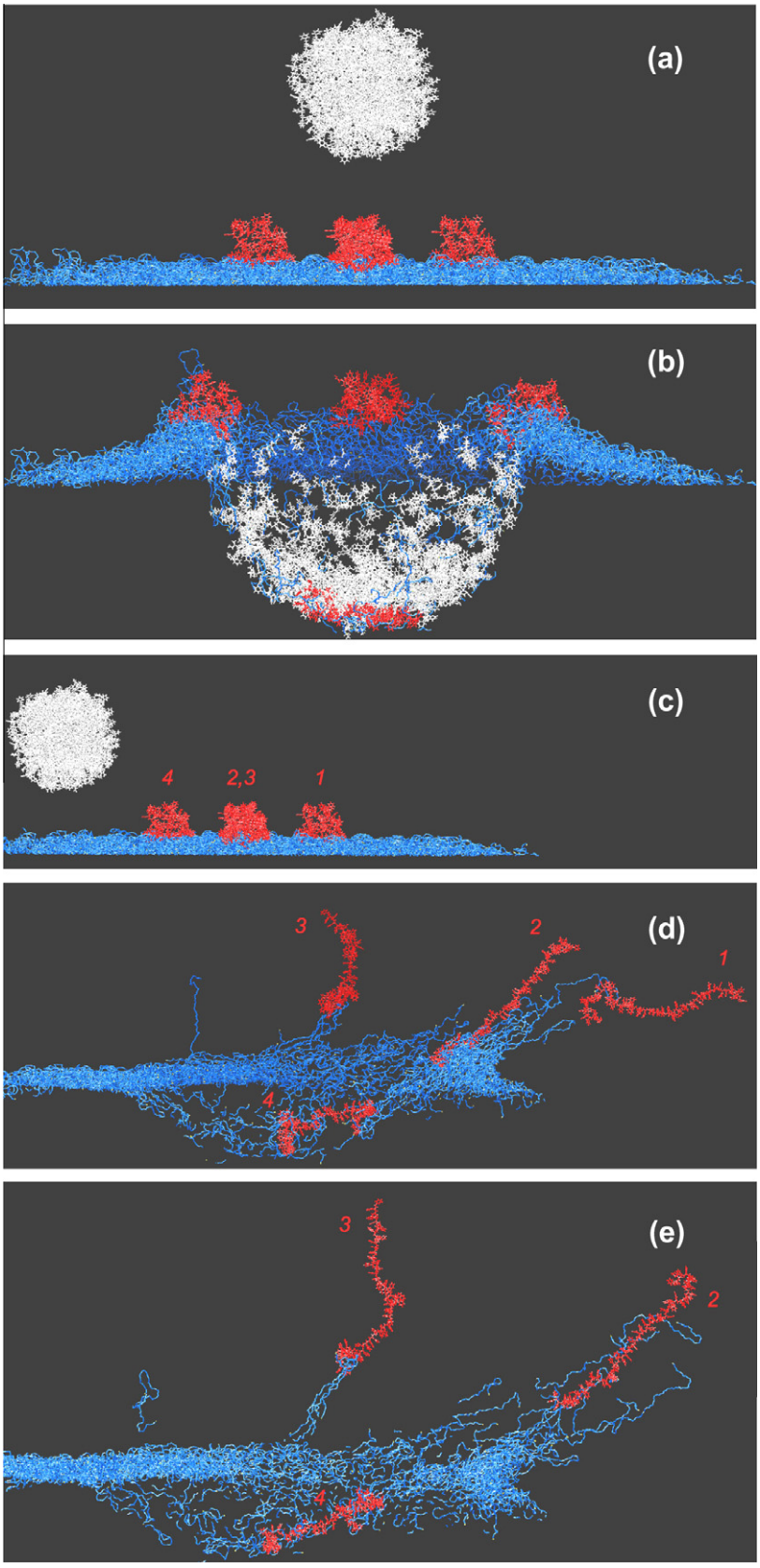

Fig. 3. Bombardment of PS61 molecules (red) adsorbed on a polymeric substrate. *Projectile:* 10 keV $(PS4)_{197}$ organic nanodrop (white); (a–b) central hit, 0° incidence, 0 and 23 ps; (c–e) side hit, 60° incidence, 0, 14 and 23 ps. In frames (d–e), the projectile atoms are omitted for clarity. (For interpretation of the references to colour in this figure legend, the reader is referred to the web version of this article.)

to the next, from 4 to 2 to 1, finally leading to a very energetic molecule 1; (ii) molecule 3 is off the projectile path and in that case, lower energies arise from the lateral development of the crater.

4. Conclusion

Our study shows that large molecules such as PS61 can be desorbed from hard and soft substrates by 10 keV massive organic clusters or nanodrops. Two different mechanisms could be identified, which lead to different balances of translational and internal kinetic energies of the desorbed molecule. For both substrates, the mechanism that is the most adequate to produce relatively 'cold' molecules is one in which the projectile washes the molecule away, so that it is entrained by the projectile constituents which are reflected from the surface. The emission angles are predicted to be around 70° irrespective of the substrate. However, the internal KEs reached on the soft polymeric substrate are generally larger than those calculated for the hard substrate.

Acknowledgments

This work was supported by the Belgian Fonds National pour la Recherche Scientifique (FNRS), the French Community of Belgium via the Concerted Research Action programme (ARC NANHYMO: convention 07/12-003) and the European Community (EC) FP7 program through the project grant CP-TP 200613-2 (''3D-Nanochemiscope''). B.J.G. acknowledges financial support from grant CHE-0910564, which is administered by the Chemistry Division of the National Science Foundation. Computational resources were provided by the academic Services and Emerging technologies (ASET). The authors are also thankful to the ASET staff for assistance with the Lion-xo and Lion-xj clusters. The theoretical and computational biophysics group of the University of Illinois at Urbana-Champaign is acknowledged for the development and free access to the visualization software VMD, used to produce Figures 2 and 3.

References

[1] G. Gillen, A. Fahey, M. Wagner, Ch. Mahoney, Appl. Surf. Sci. 252 (2006) 6537.
[2] J.S. Fletcher, S. Rabbani, A. Henderson, P. Blenkinsopp, S.P. Thompson, N.P. Lockyer, J.C. Vickerman, Anal. Chem. 80 (2008) 9058.
[3] Z. Li, S.V. Verkhoturov, E.A. Schweikert, Anal. Chem. 78 (2006) 7410.
[4] S. Ninomiya, Y. Nakata, K. Ichiki, T. Seki, T. Aoki, J. Matsuo, Nucl. Instrum. Methods Phys. Res. B 256 (2007) 493.
[5] K. Ichiki, S. Ninomiya, Y. Nakata, Y. Honda, T. Seki, T. Aoki, J. Matsuo, Appl. Surf. Sci. 255 (2008) 1148.
[6] Z. Takats, J.M. Wiseman, R.G. Cooks, J. Mass Spectrom. 40 (2005) 1261.
[7] A. Venter, P.E. Sojka, R.G. Cooks, Anal. Chem. 78 (2006) 8549.
[8] D.S. Cornett, T.D. Lee, J.F. Mahoney, Rapid Commun. Mass Spectrom. 8 (1994) 996.
[9] K. Hiraoka, K. Mori, D. Asakawa, J. Mass Spectrom. 41 (2006) 894.
[10] K. Hiraoka, D. Asakawa, S. Fujimaki, A. Takamizawa, K. Mori, Eur. Phys. J. D 38 (2006) 225.
[11] S. Ninomiya, K. Ichiki, H. Yamada, Y. Nakata, T. Seki, T. Aoki, J. Matsuo, Rapid Commun. Mass Spectrom. 23 (2009) 1601.
[12] S. Ninomiya, K. Ichiki, H. Yamada, Y. Nakata, T. Seki, T. Aoki, J. Matsuo, Rapid Commun. Mass Spectrom. 23 (2009) 3264.
[13] Y. Sakai, Y. Iijima, K. Mori, K. Hiraoka, Surf. Interface. Anal. 40 (2008) 1716.
[14] K. Hiraoka, Y. Sakai, Y. Iijima, D. Asakawa, K. Mori, Appl. Surf. Sci. 255 (2009) 8947.
[15] L. Rzeznik, B. Czerwinski, B.J. Garrison, N. Winograd, Z. Postawa, J. Phys. Chem. C 112 (2008) 521.
[16] T. Seki, T. Murase, J. Matsuo, Nucl. Instrum. Methods Phys. Res. B 242 (2006) 179.
[17] J. Matsuo, S. Ninomiya, Y. Nakata, K. Ichiki, T. Aoki, T. Seki, Nucl. Instrum. Methods Phys. Res. B 257 (2007) 627.
[18] Ch. Anders, H.M. Urbassek, R.E. Johnson, Phys. Rev. B 70 (2004) 155404.
[19] K.E. Ryan, B.J. Garrison, Anal. Chem. 80 (2008) 6666.
[20] A. Delcorte, B.J. Garrison, K. Hamraoui, Anal. Chem. 81 (2009) 6646.
[21] B.J. Garrison, Z. Postawa, Mass Spectrom. Rev. 27 (2008) 289.
[22] B.J. Garrison, P.B.S. Kodali, D. Srivastava, Chem. Rev. 96 (1996) 1327.
[23] A. Delcorte, B.J. Garrison, K. Hamraoui, Surf. Interface Anal. (2010), doi:10.1002/sia.3405.
[24] A. Delcorte, B.J. Garrison, J. Phys. Chem. C 111 (2007) 15312.
[25] M.S. Stave, D.E. Sander, T.J. Raeker, A.E. DePristo, J. Chem. Phys. 93 (1990) 4413.
[26] S.J. Stuart, A.B. Tutein, J.A. Harrison, J. Chem. Phys. 112 (2000) 6472.
[27] D.W. Brenner, O.A. Shenderova, J.A. Harrison, S.J. Stuart, B. Ni, S.B. Sinnott, J. Phys.: Condens. Matter 14 (2002) 783.
[28] K.S.S. Liu, C.W. Yong, B.J. Garrison, J. Vickerman, J. Phys. Chem. B 103 (1999) 3195.
[29] A.K. Rappé, C.J. Casewit, K.S. Colwell, W.A. Goddard III, W.M. Skiff, J. Am. Chem. Soc. 114 (1992) 10024.
[30] A. Delcorte, Sputtering and ionization basics, in: The Encyclopedia of Mass Spectrometry, in: D. Beauchemin, D. Matthews (Eds.), Elemental and Isotope Ratio Mass Spectrometry, vol. 5, Elsevier, 2010, pp. 397–411.
[31] Z. Postawa, B. Czerwinski, M. Szewcik, E.J. Smiley, N. Winograd, B.J. Garrison, Anal. Chem. 75 (2003) 4402.
[32] T. Aoki, J. Matsuo, Nucl. Instrum. Methods Phys. Res. B 257 (2007) 645.
[33] T. Aoki, J. Matsuo, Nucl. Instrum. Methods Phys. Res. B 261 (2007) 639.